High-energy photoproduction of W bosons

Kalpana J. Kallianpur*
Center for Particle Theory, University of Texas, Austin, Texas 78712
(Received 31 March 1986)

The cross sections and energy and angular distributions are calculated for the reactions $\gamma+n\to W^-+p$ and $\gamma+p\to W^++n$. Weak and electromagnetic form factors are used and an anomalous magnetic moment κ of the W boson is included. We give results for the values $\kappa=1,0,-1$.

I. INTRODUCTION

With the possibility of a high-energy photon beam at the Superconducting Super Collider the process of single-W-boson photoproduction has acquired new interest.[1] If the cross sections are sufficiently large, the reactions

$$\gamma+n\to W^-+p\ , \tag{1}$$

$$\gamma+p\to W^++n\ , \tag{2}$$

provide a means of directly measuring the trilinear gauge-boson coupling and thus the anomalous magnetic dipole moment κ of the W. The related processes

$$\mu^-+p\to\mu^-+n+W^+\ , \tag{3}$$

$$\mu^-+n\to\mu^-+p+W^-\ , \tag{4}$$

in which the W boson is likewise produced at a hadronic vertex, were considered by Fearing, Pratap, and Smith[2] and yielded results for the photoproduction reactions (1) and (2) as a special case.[3] These authors included form-factor effects at the weak and electromagnetic vertices and derived the high-energy limit of the total cross section. In the case of an elementary target, however, their expression does not simplify to the analogous formula calculated by Mikaelian[4] for a point target of variable charge Q. For $s\gg M_W{}^2$, the cross section obtained by Mikaelian is independent of Q and increases logarithmically with s except for the case $\kappa=1$, where it levels off at the constant value

$$\sigma=\sqrt{2}\,\alpha G_F\simeq 4.6\times 10^{-35}\ \text{cm}^2\ . \tag{5}$$

Although we have not derived an analytic expression for σ in this paper, Eq. (5) serves as a useful numerical check on our results.

In Sec. II we review the technique used by Fearing, Pratap, and Smith to handle the problem of gauge invariance caused by the use of realistic form factors. The same method has been employed here. The matrix element for $\gamma+n\to W^-+p$ is given in Sec. III where some additional remarks are then made on the gauge properties of the amplitude. Curves for the cross sections and energy and angular distributions are presented in Sec. IV. Finally, we discuss how uncertainty about the form of the weak Wpn vertex affects the reliability of our results.

Our calculation differs from that of Fearing, Pratap, and Smith in that we have included three instead of only two weak form factors and have been able to use the correct W-boson mass. Most importantly, although we have kept all masses in the problem and have calculated the cross section numerically, we have verified agreement with the high-energy limit (5) of Mikaelian.

II. GAUGE INVARIANCE OF THE AMPLITUDE

Given the usual electromagnetic and weak vertices, the Feynman graphs which contribute to the elastic process $\gamma+n\to W^-+p$ are those of Fig. 1. Form factors for the weak hadronic vertex are well known at least in the space-like region. Meson-exchange diagrams, for which the vertex structures are much more uncertain, are expected to contribute virtually nothing to W photoproduction. In particular the one-pion-exchange graph (Fig. 2) was considered by Bander[5] and later explicitly evaluated by Fearing, Pratap, and Smith,[3] who found its contribution to be negligible except very near threshold. The ρ-meson-exchange diagram of Fig. 2 was similarly estimated to be small at high energies.[3] We have therefore considered only the standard channels of W and nucleon exchange.

We incorporate strong-interaction effects through phenomenological form factors as usual. Since inclusion of weak form factors results in the matrix element losing explicit gauge invariance, an extra term must be added to preserve it. This is analogous to the case of pion electroproduction where a term proportional to k^μ/k^2 is added to the amplitude for the same reason. Electromagnetic form factors, of course, pose no such difficulty in photoproduction as they are simply given by their static values.

The method used to restore explicit gauge invariance is explained in detail in Fearing, Pratap, and Smith, but we

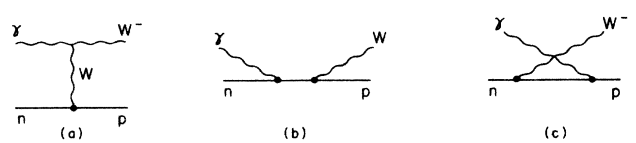

FIG. 1. Feynman diagrams for the process $\gamma+n\to W^-+p$. The circles indicate vertices where form factors are included.

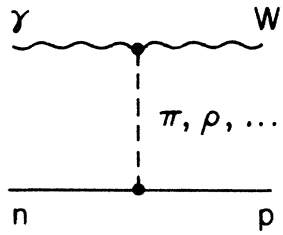

FIG. 2. Meson-exchange diagrams with negligible contributions at high energies.

outline it here for completeness. For the purpose of illustration, we will describe the *Wpn* coupling [Fig. 3(c)] by only two weak form factors, vector and axial vector:

$$\Gamma_\mu^{WNN'}(p_1,p_2)=\frac{-ig}{2\sqrt{2}}\cos\theta_C(F_V^1\gamma_\mu+F_A\gamma_\mu\gamma_5) .$$

F_V^1 and F_A are functions of $q^2=(p_2-p_1)^2$. Because the weak form factors in diagram (a) of Fig. 1 are evaluated at values of q^2 different from those in (b) and (c), it can easily be checked (Sec. III) that restoring gauge invariance to the total W photoproduction amplitude is equivalent to making each diagram gauge invariant by itself. Hence the following procedure is carried out for each of the Feynman graphs separately, although it will prove instructive to examine the gauge invariance of the amplitude as a whole as is done in the next section.

As an example, consider the contribution of diagram (c). The matrix element is given by

$$M_3=\frac{-ieg}{2\sqrt{2}}\cos\theta_C M_3^{\alpha\beta}\epsilon_\alpha(k)\epsilon_\beta^*(k')$$

with

$$M_3^{\alpha\beta}=\bar{u}(p_2)\left[\gamma^\alpha+\frac{i\kappa^p}{2M}\sigma^{\alpha\nu}k_\nu\right]\times\frac{1}{\not{p}_2-\not{k}-M}(F_V^1\gamma^\beta+F_A\gamma^\beta\gamma_5)u(p_1) , \quad (6)$$

where $\epsilon_\alpha(k)$ and $\epsilon_\beta(k')$ are the photon and W polarization vectors, respectively, M and κ^p the mass and anomalous magnetic moment of the proton, and $\gamma^\alpha+(i\kappa^p/2M)\sigma^{\alpha\nu}k_\nu$ the proton-proton-physical photon coupling.

$$\sigma^{\mu\nu}\equiv(i/2)[\gamma^\mu,\gamma^\nu] .$$

To test M_3 for invariance, contract $M_3^{\alpha\beta}\epsilon_\beta^*(k')$ with k_α:

$$k_\alpha M_3^{\alpha\beta}\epsilon_\beta^*(k')=\bar{u}(p_2)(F_V^1\gamma^\beta+F_A\gamma^\beta\gamma_5)u(p_1)\epsilon_\beta^*(k') . \quad (7)$$

We must therefore add a term $\Delta M_3^{\alpha\beta}$ to $M_3^{\alpha\beta}$ such that

$$k_\alpha(M_3^{\alpha\beta}+\Delta M_3^{\alpha\beta})\epsilon_\beta^*(k')=0 \quad (8)$$

in order for the amplitude corresponding to diagram (c) to be gauge invariant. Consider first the vector part of $\Delta M_3^{\alpha\beta}$, which can be expanded in terms of γ^β and of any three independent four-vectors A^α, B^α, C^α of the problem:

$$\Delta M_3^{\alpha\beta}=F_V^1\bar{u}(p_2)(\alpha' A^\alpha+\beta' B^\alpha+\gamma' C^\alpha)u(p_1)+\Delta\tilde{M}^{\alpha\beta} \quad (9)$$

where α', β', γ' are arbitrary scalar coefficients and $k_\alpha\Delta\tilde{M}^{\alpha\beta}=0$. The gauge invariance condition (8) then requires

$$\alpha' k\cdot A+\beta' k\cdot B+\gamma' k\cdot C=1 ; \quad (10)$$

i.e., the scalar coefficients must have singularities in k. Redefining $\alpha'=\alpha/k\cdot A$, $\beta'=\beta/k\cdot B$, and $\gamma'=\gamma/k\cdot C$ yields the constraint

$$\alpha+\beta+\gamma=1 . \quad (11)$$

With the exception of this condition, the choice of α, β, γ, A, B, C is completely arbitrary. Note that terms proportional to $\bar{u}(p_2)\gamma^\alpha(k\cdot\gamma)\gamma^\beta u(p_1)$ and those with momentum-dependent coefficients may be absorbed into the explicitly gauge invariant $\Delta\tilde{M}^{\alpha\beta}$, which must necessarily be neglected. α, β, and γ are thus taken to be constants.

We now state the particular choice of parameters made in this paper. Since the singularities in k of α', β' and γ' depend on the choice of A,B,C, it seems desirable to pick these four-vectors so that only singularities already present in M will occur in $\Delta M_1^{\alpha\beta}$, $\Delta M_2^{\alpha\beta}$, and $\Delta M_3^{\alpha\beta}$, i.e., so that no new singularities will be introduced into the amplitude via $\Delta M_{\text{tot}}^{\alpha\beta}$. Defining $A^\mu=2k'^\mu$, $B^\mu=-2p_1^\mu$, $C^\mu=-2p_2^\mu$ would ensure this, and, in fact, is the choice made by Fearing, Pratap, and Smith[2,3] with small constant coefficients. Their results indicate a relative insensitivity to the form of the added terms: with $|\alpha|$, $|\beta|$, $|\gamma|\leq 1$, variation of these parameters changed the total photoproduction cross section by only about 10%. For W production via muon beams, σ varied by at most 20% for small coefficients, with the minimum cross section for all $|\alpha|$, $|\beta|$, $|\gamma|<\infty$ occurring when $\alpha=1$ and $\beta=\gamma=0$. This last result agrees with what might be expected; in the case where only the W pole survives in ΔM, the extra singularity added to preserve gauge invariance is very far from the physical region because q^2 is negative and M_W^2 is large. With this justification, we have chosen to keep only the W propagator singularity in ΔM_1 ΔM_2, and

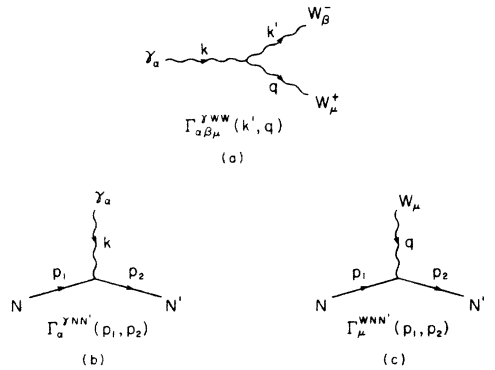

FIG. 3. Weak and electromagnetic vertices defined in Eqs. (13), (14), and (16).

ΔM_3, constraining the relevant coefficient to be unity by Eq. (11). All results presented in this paper are calculated for this definition of $A^\mu=-2k'^\mu$, $\alpha=1$, and $\beta=\gamma=0$. Further remarks on the form of ΔM are made in Sec. III once the entire matrix element has been given.

III. MATRIX ELEMENT

The interactions used to write down the amplitude for $\gamma+N\to W+N'$ are those of the standard model[6] except for the $WW\gamma$ coupling, for which we take[7]

$$\mathcal{L}=\frac{igg'}{(g^2+g'^2)^{1/2}}A^\nu[(\partial_\mu W_\nu^+-\partial_\nu W_\mu^+)W^\nu-(\partial_\mu W_\nu-\partial_\nu W_\mu)W^{\mu+}-\kappa\partial_\mu(W^{\mu+}W_\nu-W^\mu W_\nu^+)] \tag{12}$$

in order to accommodate an arbitrary anomalous magnetic moment κ of the W boson. g and g' are the usual gauge couplings:

$$g=\frac{e}{\sin\theta_W},\quad g'=g\tan\theta_W,$$

where e is the electric charge with $\alpha=e^2/4\pi=\frac{1}{137}$. The three-gauge-boson vertex, Fig. 3(a), is then

$$\Gamma^{\gamma WW}_{\alpha\beta\mu}(k,k',q)=-ie[g_{\mu\beta}(k'-q)_\alpha-g_{\beta\alpha}(k'+\kappa k)_\mu+g_{\alpha\mu}(\kappa k+q)_\beta]\,. \tag{13}$$

The standard coupling is recovered from Eqs. (12) and (13) when $\kappa=1$.

Diagrams 1(a)–1(c) contain the weak and electromagnetic vertices shown in Fig. 3. The electromagnetic hadronic vertex has the standard form

$$\Gamma^{\gamma NN'}_\alpha(p_1,p_2)=-ie\left[f_1^N(k^2)\gamma_\alpha+\frac{i\kappa^N}{2M}f_2^N(k^2)\sigma_{\alpha\nu}q^\nu\right], \tag{14}$$

where κ^N is the nucleon anomalous magnetic moment, and

$$f_1^p(0)=f_2^p(0)=f_2^n(0)=1,\quad f_1^n(0)=0\,.$$

The weak proton-neutron-W coupling of Fig. 3(c) can be parametrized most generally by

$$\Gamma^{WNN'}_\mu(p_1,p_2)=\frac{-ig\cos\theta_C}{2\sqrt{2}}[f_1(q^2)\gamma_\mu+if_2(q^2)\sigma_{\mu\nu}q^\nu+f_3(q^2)q_\mu+g_1(q^2)\gamma_\mu\gamma_5+ig_2(q^2)\sigma_{\mu\nu}q^\nu\gamma_5+g_3(q^2)\gamma_5 q_\mu] \tag{15}$$

with $g^2/8M_W{}^2=G_F/\sqrt{2}$, where M_W is the W-boson mass and G_F the Fermi constant. For spacelike $q^2=(p_2-p_1)^2$, the conserved-vector-current hypothesis requires $f_3=0$, as well as

$$f_1(q^2)=f_1^p(q^2)-f_1^n(q^2),\quad f_2(q^2)=\frac{1}{2M}[\kappa^p f_2^p(q^2)-\kappa^n f_2^n(q^2)]\,,$$

since the weak current, its conjugate, and the isovector part of the electromagnetic current form an isospin triplet. Neutron β decay gives $g_1(0)=-1.25$, and the absence of observed second-class currents thereof implies $g_2=0$. For simplicity we neglect the g_3 term and rewrite Eq. (15) as

$$\Gamma^{WNN'}_\mu(q)=\frac{-ig\cos\theta_C}{2\sqrt{2}}\left[F_V^1(q^2)\gamma_\mu+F_A(q^2)\gamma_\mu\gamma_5+\frac{i\xi F_V^2(q^2)}{2M}\sigma_{\mu\nu}q^\nu\right],\quad \xi\equiv\kappa^p-\kappa^n \tag{16}$$

so that the vector form factors are normalized to one:

$$F_V^1(0)=F_V^2(0)=1,\quad F_A(0)=-1.25\,.$$

The matrix element for $\gamma(k,\alpha)+n(p_1)\to W^-(k',\beta)+p(p_2)$ is

$$M^{\rm tot}=\frac{-ieg}{2\sqrt{2}}\cos\theta_C(M_1+M_2+M_3)^{\alpha\beta}\epsilon_\alpha(k)\epsilon^*_\beta(k')\,, \tag{17}$$

where M_1, M_2, and M_3, the amplitudes corresponding to graphs 1(a)–1(c), are

$$M_1^{\alpha\beta}=[g^{\mu\beta}(k'-q)^\alpha-g^{\beta\alpha}(k'+\kappa k)^\mu+g^{\alpha\mu}(\kappa k+q)\beta]\frac{\left[-g_{\mu\nu}+\dfrac{q_\mu q_\nu}{M_W{}^2}\right]}{q^2-M_W{}^2}$$

$$\times\bar u(p_2)\left[F_V^1(t)\gamma^\nu+F_A(t)\gamma^\nu\gamma_5+\frac{i\xi}{2M}F_V^2(t)\sigma^\nu_\rho q^\rho\right]u(p_1)\,,$$

$$M_2^{\alpha\beta}=\bar{u}(p_2)\left[F_V^1\gamma^\beta+F_A\gamma^\beta\gamma_5-\frac{i\xi}{2M}F_V^2\sigma^{\beta\nu}k'_\nu\right]\frac{1}{\not p_1+\not k-M}\left[f_n(0)\gamma^\alpha+\frac{i\kappa^n}{2M}\sigma^{\alpha\nu}k_\nu\right]u(p_1)\,, \tag{18}$$

$$M_3^{\alpha\beta}=\bar{u}(p_2)\left[f_p(0)\gamma^\alpha+\frac{i\kappa^p}{2M}\sigma^{\alpha\nu}k_\nu\right]\frac{1}{\not p_2-\not k-M}\left[F_V^1\gamma^\beta+F_A\gamma^\beta\gamma_5-\frac{i\xi}{2M}F_V^2\sigma^{\beta\nu}k'_\nu\right]u(p_1)\,.$$

Here

$t=q^2=(k-k')^2$ and $F_V^1\equiv F_V^1(M_W{}^2)$, etc.

Although the electromagnetic form factors are evaluated at $k^2=0$, f_1^p and f_1^n have not been replaced by their static values here in order that we may easily obtain the amplitude for $\gamma+p\to W^++n$ by letting $f_1^p(0)\leftrightarrow f_1^n(0)$ and $M_1\to -M_1$ in the above.

Now we use the method of the previous section to make M_1, M_2, M_3 each explicitly gauge invariant. After contracting each amplitude with k and adding to it a term with a W-propagator singularity as described earlier, we have

$$k_\alpha M_{\rm tot}^{\alpha\beta}\epsilon_\beta^*(k')=\bar{u}(p_2)\Big\{[-f_1^p(0)F_V^1+f_1{}^n(0)F_V^1+F_V^1(t)]\gamma^\beta+[-f_1^p(0)F_A+f_1^n(0)F_A+F_A(t)]\gamma^\beta\gamma_5$$
$$-\frac{i\xi}{2M}[-f_1^p(0)F_V^2+f_1^n(0)F_V^2+F_V^2(t)]\sigma^{\beta\nu}k'_\nu-\frac{i\xi}{2M}F_V^2(t)\sigma^{\beta\nu}k_\nu\Big\}u(p_1)\epsilon_\beta^*(k') \tag{19}$$

and

$$\Delta M_{\rm tot}^{\alpha\beta}\epsilon_\alpha(k)\epsilon_\beta^*(k')=-\frac{2k'^\alpha}{t-M_W{}^2}\bar{u}(p_2)\Big\{[f_1^p(0)F_V^1-f_1^n(0)F_V^1-F_V^1(t)]\gamma^\beta+[f_1^p(0)F_A-f_1^n(0)F_A-F_A(t)]\gamma^\beta\gamma_5$$
$$-\frac{i\xi}{2M}[f_1^p(0)F_V^2-f_1^n(0)F_V^2-F_V^1(t)]\sigma^{\beta\nu}k'_\nu-\frac{i\xi}{2M}F_V^2(t)\sigma^{\beta\nu}k_\nu\Big\}u(p_1)\epsilon_\alpha(k)\epsilon_\beta^*(k')\,. \tag{20}$$

Because the forms of F_V^1, F_V^2, and F_A are almost unknown in the timelike region, particularly for values of t as large as $M_W{}^2$, we have considered two different possibilities for their behavior. Results are presented for constant weak timelike form factors, i.e., with their static ($t=0$) values, as well as for dipole timelike form factors falling off exactly as is in the spacelike domain. The dipole parametrization of the weak form factors is given below:

$$F_V^1(q^2)=\left[1-\frac{q^2}{4M^2}\right]^{-1}\left[G_E^V(q^2)-\frac{q^2}{4M^2}G_M^V(q^2)\right],$$
$$\xi F_V^2(q^2)=\left[1-\frac{q^2}{4M^2}\right]^{-1}[G_M^V(q^2)-G_E^V(q^2)]\,,$$
$$G_E^V(q^2)=\left[1-\frac{q^2}{m_V{}^2}\right]^{-2}, \tag{21}$$
$$G_M^V(q^2)=(1+\xi)\left[1-\frac{q^2}{m_V{}^2}\right]^{-2},$$
$$F_A(q^2)=-1.25\left[1-\frac{q^2}{m_A{}^2}\right]^{-2}.$$

$m_V=0.84$ GeV, the electromagnetic dipole value, and in F_A we take $m_A=0.95$ GeV (Ref. 8). We have used $M_W=82.42$ GeV, $M=1$ GeV and $\kappa^p=1.79$, $\kappa^n=-1.91$ in the calculation.

While imposing gauge invariance on M_1, M_2, M_3 individually results in only the constraint (11) on an added term of the form (9), consideration of the total amplitude suggests another desired property of $\Delta M_{\rm tot}$. With only F_V^1 and F_A included in $\Gamma^{WNN'}$, the sum $M_{\rm tot}$ of the three diagrams is obviously gauge invariant by Eq. (19) for constant form factors. Therefore, in this case $\Delta M_{\rm tot}$ must go smoothly to zero as the form factors approach their static values. Equation (20) satisfies this condition. We note that $M_{\rm tot}$ is no longer gauge invariant for constant form factors when F_V^2 is included.

The analogy with pion electroproduction now becomes more illuminating. In $e+N\to e+N'+\pi$, where the amplitude is similarly gauge invariant for static form factors, the term $\propto k^\mu/k^2$ which restores gauge invariance is multiplied by a combination of form factors that vanishes at $k^2=0$. For our process, however, the coefficient does not vanish at $q^2=0$ so that a term of the same form would introduce a singularity which is in the physical region and not present in the original amplitude. Although a term $\propto q^\mu/q^2$ is thus ruled out when only F_V^1 and F_A are included, the form of $\Delta M_{\rm tot}$ given by Eq. (20) has a pole with zero residue exactly as does the term added in pion electroproduction. It has already been mentioned that the results of Fearing, Pratap, and Smith are fairly uniform as long as the residue of the extra unphysical pole is small. For W photoproduction the $\Delta M_{\rm tot}$ of Eq. (20) is therefore probably the optimal choice as the residue of its pole is identically zero when $F_V^2(t)=0$ and is small otherwise.

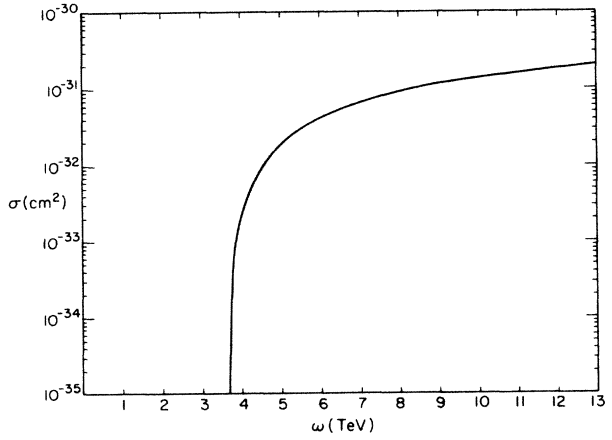

FIG. 4. Total cross section for $\gamma+n\to W^-+p$ as a function of the laboratory energy ω of the photon, with no form factors included and $\kappa=-1, 0, 1$. The curve with dipole spacelike and constant timelike form factors is essentially identical.

IV. RESULTS

In this section the total cross sections and angular and energy distributions for $\gamma+n\to W^-+p$ are presented and discussed. Results are given both with and without the use of weak form factors and for different values of the W anomalous magnetic moment κ. The integration over the energy of the final nucleon was done numerically.

We begin by looking at the contributions of the three graphs for different cases. Without form factors, diagrams (b) and (c) dominate the cross section in qualitative agreement with Fearing, Pratap, and Smith, who separated the contributions of the charge and magnetic moment parts of these graphs and found the latter to be larger by ≥ 2 orders of magnitude. Thus in this case κ has virtually no effect on σ. Inclusion of dipole spacelike and constant timelike form factors yields results essentially identical to those with no form factors since diagrams (b) and (c) remain undamped. Only when dipole timelike form factors are included does diagram (a) become significant. This is due to the fact that the contributions of (b) and (c) are multiplied by a factor proportional to the squares of the form factors evaluated at $M_W{}^2$; as we shall see, even for timelike form factors falling off more slowly than a dipole, this constant factor effectively eliminates (b) and (c). The cross section is then given by diagram (a) and the value of κ is crucial.

Cross sections and distributions for $\gamma+p\to W^++n$ were found to be almost identical to those of $\gamma+n\to W^-+p$, except just above threshold where σ for a

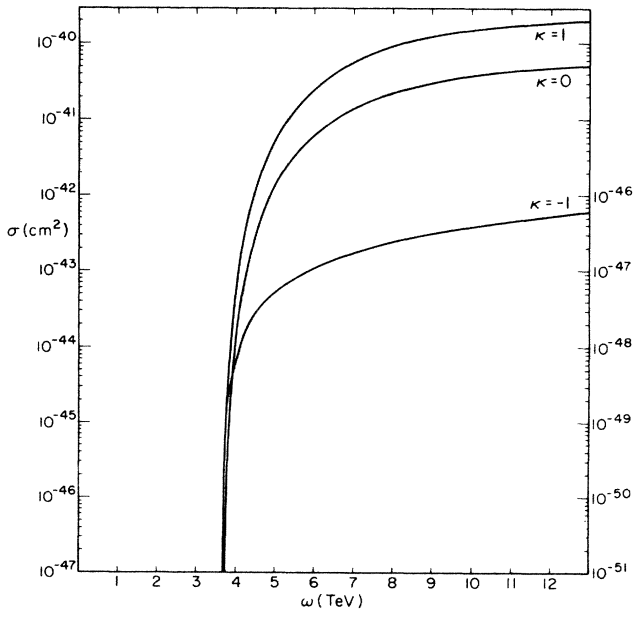

FIG. 5. Total cross sections for $\gamma+n\to W^-+p$ as a function of photon beam energy ω, with dipole form factors included. For $\kappa=-1$ read the scale on the right axis.

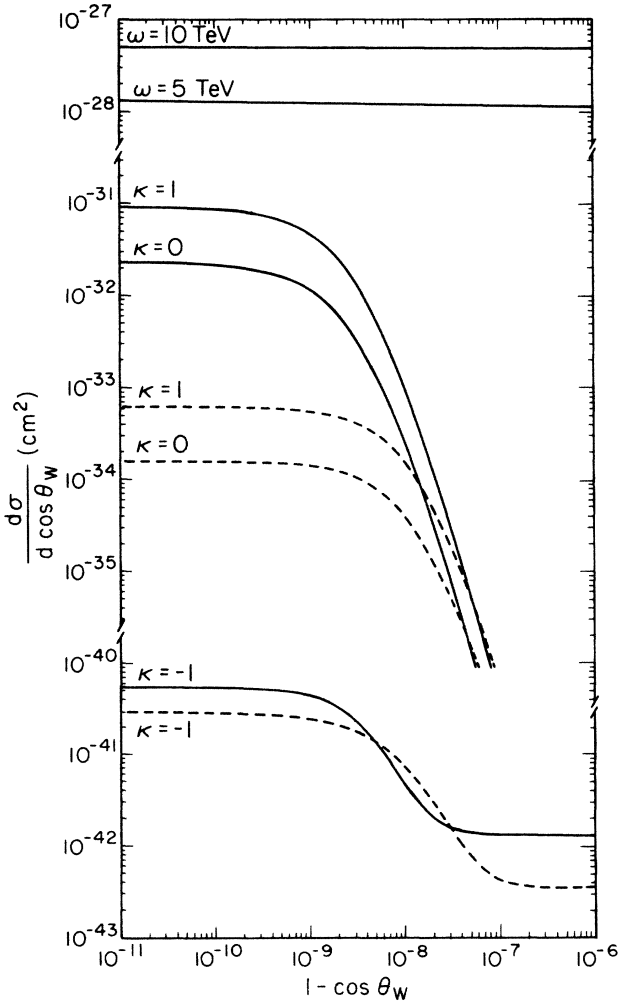

FIG. 6. The differential cross sections $d\sigma/d\cos\theta_W^{\rm lab}$ for $\gamma+n\to W^-+p$ with photon energies $\omega=5$ TeV and $\omega=10$ TeV. The upper curves correspond to no form factors (or constant timelike form factors) and $\kappa=-1, 0, 1$. The lower curves correspond to dipole form factors, with dashed curves for $\omega=5$ TeV and solid ones for $\omega=10$ TeV. Note the two changes of scale.

proton target is larger by $\lesssim 4\%$. For no form factors, this confirms the finding of Fearing, Pratap, and Smith that the magnetic moment parts of diagrams (b) and (c) are approximately equal and that the leading terms of the cross section are symmetric under the interchange $p \leftrightarrow n$. When dipole form factors are included this result is obvious because the only contribution comes from (a) and is independent of the type of target nucleon.

The total cross section for $\kappa = -1$, 0, 1 with no form factors or with dipole spacelike and constant timelike form factors is plotted in Fig. 4. σ for $\kappa = 1$, 0, -1 with dipole spacelike and timelike form factors is shown in Fig. 5. At large photon beam energy ω, the cross section in Fig. 4 is several orders of magnitude greater than the high-energy limit $\sigma \sim 10^{-35}$ cm^2 for a pointlike target. This arises from the dominance of the κ^p and κ^n terms; by explicitly setting these contributions to zero, the limit (5) is achieved. The inclusion of dipole form factors severely damps σ by about 9 orders of magnitude. Note that in this case the cross section for $\kappa = -1$ is greatly suppressed relative to those with $\kappa = 1$ and $\kappa = 0$. The contribution of diagram (a) goes[2,3] essentially as $(1+\kappa)^2$, so that σ for $\kappa = 1$ is about 4 times larger than σ for $\kappa = 0$, etc., with W exchange contributing almost nothing to the process when $\kappa = -1$.

The angular distribution $d\sigma/d\cos\theta_W$ of the W boson is given in Fig. 6 for photon beam energies of 5 and 10 TeV. The curves for no form factors (or dipole spacelike form factors) are nearly flat, while those with dipole timelike form factors included are strongly forward peaked and become more so as the photon energy increases. In Fig. 6 we have also shown $d\sigma/d\cos\theta_W$ with dipole form factors for $\omega = 5$ and 10 TeV and $\kappa = -1$, 0,1. $d\sigma/d\cos\theta_W$ for $\kappa = -1$ is relatively flat even with dipole timelike form factors; in this case the effect of diagram (a) is canceled and (b) and (c), though severely reduced by a constant scale factor, dominate just as in the absence of form factors.

From the energy distributions of the final nucleon (Fig. 7) we see that the primary effect of dipole form factors is again to change the shape of $d\sigma/dE_p$ from fairly flat to very strongly peaked at small E_p, except when $\kappa = -1$ for the same reason as before. Without form factors, $d\sigma/dE_p$ becomes slightly more peaked at small E_p as ω increases, but when dipole form factors are used the shape of these distributions is more or less independent of the photon energy.

Finally, we wish to examine how lack of information about timelike weak form factors might affect our results. To check how σ changes when these form factors fall off

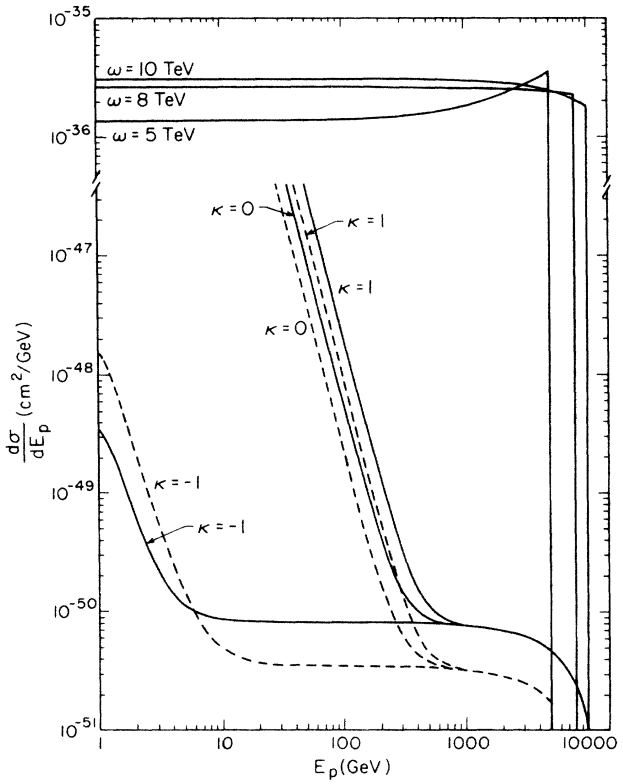

FIG. 7. The differential cross sections $d\sigma/dE_p$ for $\gamma + n \to W^- + p$. The upper curves correspond to no form factors (or constant timelike form factors) and $\kappa = -1$, 0, 1. The lower curves correspond to dipole form factors with photon energy $\omega = 5$ TeV (dashed curves) and $\omega = 10$ TeV (solid curves). Note the change of scale.

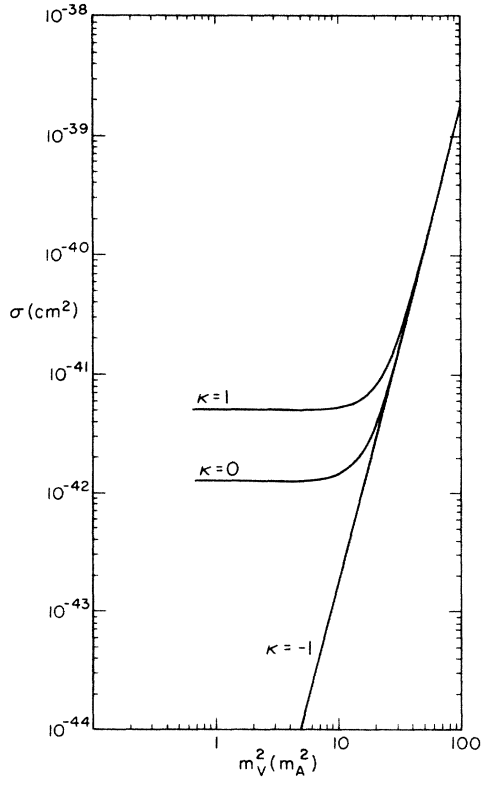

FIG. 8. Total cross sections for $\gamma + n \to W^- + p$ with photon energy $\omega = 5$ TeV, as a function of the parameter $m_V{}^2$ ($m_A{}^2$) of weak form factors in the timelike region where m_V has been set equal to m_A [Eq. (21)]. $m_V{}^2 = 0.71$ GeV^2 corresponds to the electromagnetic dipole. Electromagnetic and dipole spacelike form factors have been included.

less rapidly than an electromagnetic dipole, we have set $m_V = m_A$ in Eqs. (21) for timelike form factors and have plotted the cross section for $\omega = 5$ TeV as a function of m_V in Fig. 8. For $\kappa = 0$ or 1 σ is uniform provided that the form factors fall off at almost any reasonable rate; only when $m_V^2 \geq 8$ GeV^2, far above the electromagnetic dipole value 0.71 GeV^2, do diagrams (b) and (c) begin to contribute once more to the cross section. When $\kappa = -1$, however, σ is extremely sensitive to m_V^2, suggesting that for this value of the W anomalous magnetic moment the shapes of the curves are more reliable than their magnitudes. Such a result is to be expected since the contribution of diagram (a) is negligible in this case.

In summary, realistic form factors drastically reduce the size of the cross section without significantly changing its shape in the region of interest. The energy and angular distributions in contrast become strongly peaked at small E_p and at large $\cos\theta_W$, except for the case $\kappa = -1$ where they remain relatively flat. The W boson emerges at extreme forward angles and carries off most of the energy. A luminosity of 0.6×10^{39} cm^{-2}/yr for the proposed 10-TeV photon beam[1] yields an event rate of 0.09/yr for $\kappa = 1$, clearly ruling out elastic W photoproduction as a possible means of measuring κ at the SSC.

ACKNOWLEDGMENTS

I would like to thank Duane Dicus for suggesting this problem and providing guidance throughout, and for reading the manuscript carefully and making several useful suggestions. I also thank Stephen Eubank for invaluable help in computer programming.

*Present address: Department of Physics, University of Wisconsin, Madison, WI 53706.

[1] M. J. Tannenbaum, talk given at the 1984 Superconducting Super Collider Fixed Target Workshop, Fermi National Accelerator Laboratory (unpublished).

[2] H. W. Fearing, M. Pratap, and J. Smith, Phys. Rev. D 5, 158 (1972).

[3] H. W. Fearing, M. Pratap, and J. Smith, Phys. Rev. D 5, 177 (1972).

[4] K. O. Mikaelian, Phys. Rev. D 17, 750 (1978).

[5] M. Bander, Nucl. Phys. **41**, 47 (1963).

[6] S. Weinberg, Phys. Rev. Lett. **19**, 1264 (1967); **27**, 1688 (1971); A. Salam, in *Elementary Particle Theory: Relativistic Groups and Analyticity (Nobel Symposium No. 8)*, edited by N. Svartholm (Almqvist and Wiksell, Stockholm, 1968), p. 367.

[7] W. A. Bardeen, R. Gastmans, and B. Lautrup, Nucl. Phys. **B46**, 319 (1972).

[8] W. A. Mann *et al.*, Phys. Rev. Lett. **31**, 844 (1973); T. E. Kim, P. Langacker, M. Levine, and H. H. Williams, Rev. Mod. Phys. **53**, 211 (1981); P. Q. Hung and J. J. Sakurai, Annu. Rev. Nucl. Part. Sci. **31**, 375 (1981).